JPE 15-6-7

http://dx.doi.org/10.6113/JPE.2015.15.6.1480
ISSN(Print): 1598-2092 / ISSN(Online): 2093-4718

A Simple Structure of Zero-Voltage Switching (ZVS) and Zero-Current Switching (ZCS) Buck Converter with Coupled Inductor

Xinxin Wei†, Ciyong Luo*, Hang Nan*, and Yinghao Wang*

†,*State Key Laboratory of Power Transmission Equipment & System Security and New Technology, Chongqing University, Chongqing, China

Abstract

In this paper, a revolutionary buck converter is proposed with soft-switching technology, which is realized by a coupled inductor. Both zero-voltage switching (ZVS) of main switch and zero-current switching (ZCS) of freewheeling diode are achieved at turn on and turn off without using any auxiliary circuits by the resonance between the parasitic capacitor and the coupled inductor. Furthermore, the peak voltages of the main switch and the peak current of the freewheeling diode are significantly reduced by the coupled inductor. As a result, the proposed converter has the advantages of simple circuit, convenient control, low consumption and so on. The detailed operation principles and steady-state analysis of the proposed ZVS-ZCS buck converter are presented, and detailed power loss analysis and some simulation results are also included. Finally, experimental results based on a 200-W prototype are provided to verify the theory and design of the proposed converter.

Key words: Buck converter, Coupled inductor, Soft switching, Zero-current switching (ZCS), Zero-voltage switching (ZVS)

I. INTRODUCTION

Buck converters have been widely used in the industry, especially in low-voltage and high-current applications. With the development of power electronics technology, it is imperative to demand small-sized, lightweight, and high-reliability qualities and power density for the converters. To achieve these, high-switching frequency is used to the converters. However, the increase of switching losses results in an increase of switching frequency, if converters operate under hard-switching conditions, and consequently, adversely affects the efficiency of the overall circuits. Then, soft-switching techniques are applied to the converters, which will considerably decrease switching losses, improve efficiency, and enhance stability. In addition, soft switching can reduce electromagnetic interference and the size of heat sinks.

In recent years, to achieve soft switching, many researchers have proposed a great amount of methods. Zero-voltage switching (ZVS) and zero-current switching (ZCS) are the most popular methods of soft switching, which can be realized by quasi-resonant circuits [1]-[11]. While some auxiliary components are normally added to the converter to obtain quasi-resonant circuits, such as switches, diodes, inductors, capacitors and so on. In [4], [5], the loss of main switch is decreased by the quasi-resonant circuits, but some additional elements work under hard-switching conditions, which generate a large amount of power losses. Therefore, it is not obvious that the total efficiency of the converters has improved. High-peak voltage or current of the main power switches and the diodes also happened [6]-[8]. Consequently, higher ranks of devices must be adopted for the converters, and additional power losses will also be generated. In any case, the control algorithm is more complicated than that of conventional pulse width modulation converters because of the auxiliary switches being added to the converters.

Coupled inductor also has been applied to the conventional converters in the early researches to realize soft switching that can obtain high efficiency [12]-[18]. In [13], even though the efficiency of the proposed converter can be improved under heavy-load conditions, it is worse than that of the conventional

Manuscript received Mar. 12, 2015; accepted Jun. 20, 2015
Recommended for publication by Associate Editor Jung-Wook Roh.
†Corresponding Author: 370423647@qq.com
Tel: +86-23-6510-2434, Fax: +86-23-6510-2441, Chongqing University
*State Key Laboratory of Power Transmission Equipment & System Security and New Technology, Chongqing University, China

ones under light-load conditions because the auxiliary circuits generate a large number of additional conduction losses at light load. To make the main switch achieve ZCS condition, it is demanding the converter to operate under discontinuous conduction mode in [15]. When the current of the main small inductor is discontinuous, the coupled inductor can supply power to the loads. However, the additional diode and the copper losses of the coupled inductor itself have an adverse effect on the total efficiency. Although the topology of the buck converter in [17] is very simple, the switching frequency is variable, which makes the control method much more complex.

In this paper, a revolutionary control method is proposed to achieve soft switching, based on the extended topology in [17]. The topology of proposed ZVS-ZCS buck converter is shown in Fig. 1. As is evident from the figure, the filter inductor of the conventional converter is replaced by a coupled inductor. The main power switch can work under ZVS conditions at turn on and turn off. The freewheeling diode can also operate under ZCS conditions at turn on and turn off, i.e., soft switching of the proposed converter can be achieved. Moreover, there are not any auxiliary components or quasi-resonant circuit branches, which often generate additional power dissipations. Hence, the control method is very facile, similar to that of the conventional converter. A 200-W prototype is also built to verify the theory of the proposed converter.

The rest of this paper is organized as follows: Section II takes a brief description of the proposed converter, then the key waveforms and the equivalent circuits of each mode are presented. In Section III, the requirements of achieving soft switching and the specific parameter design of proposed converter are given. Section IV presents some simulation results and the detailed power dissipations. In Section V, the experimental results are obtained to illustrate the proposed converter. Finally, some conclusions are included in Section VI.

II. Converter Description and Operating Principles

A. Description of the Converters

The topology of proposed ZVS-ZCS buck converter is shown in Fig. 1. S_1 is the power MOSFET, and D_S is an anti-parallel diode that integrates in the power MOSFET. D_1 is the freewheeling diode, C_1 is the filter capacitor, and C_r is the parasitic capacitor. L_1 and L_2 are tightly coupled on the same ferrite core that constitutes a coupled inductor. The coupled inductor L_1 is so small that its current can be bidirectional. Because of the resonance between the parasitic capacitor C_r and the coupled inductor L_1, switch S_1 can be turned on and off under ZVS conditions. The coupled inductor L_2 creates ZCS conditions for the freewheeling diode D_1 that is turned on and off.

B. Operation Principles and Analysis

The operation processes of switching circuits are repeated by the switching period, and any particular time during the switching period can be chosen as a starting point to analyze them. The analysis processes can be simplified by selecting the appropriate starting point. This paper chose a starting point at switch S1 turned-off moment. The key ideal waveforms of the proposed ZVS-ZCS buck converter are shown in Fig. 2. The operation of the proposed converter in one switching period can be divided into six, and the equivalent circuits of each stage are presented in Fig. 3. The detailed analyses of each mode are described as follows:

1) Mode 1 [t_0-t_1, Fig. 3(a)]: The freewheeling diode D_1 turns on in this interval. Before t_0, the switch S_1 is turned on, and u_{Cr} is equal to zero. The freewheeling diode D_1 is turned off, and i_2 is also equal to zero. At t_0, switch S_1 turns off under a ZVS

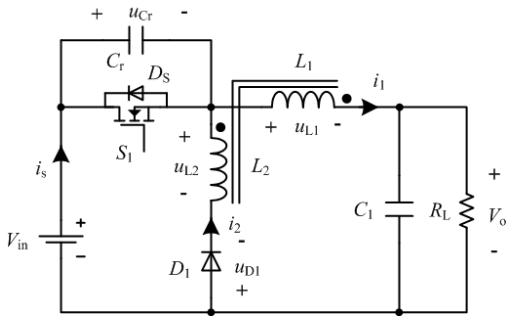

Fig. 1. The topology of proposed ZVS-ZCS buck converter.

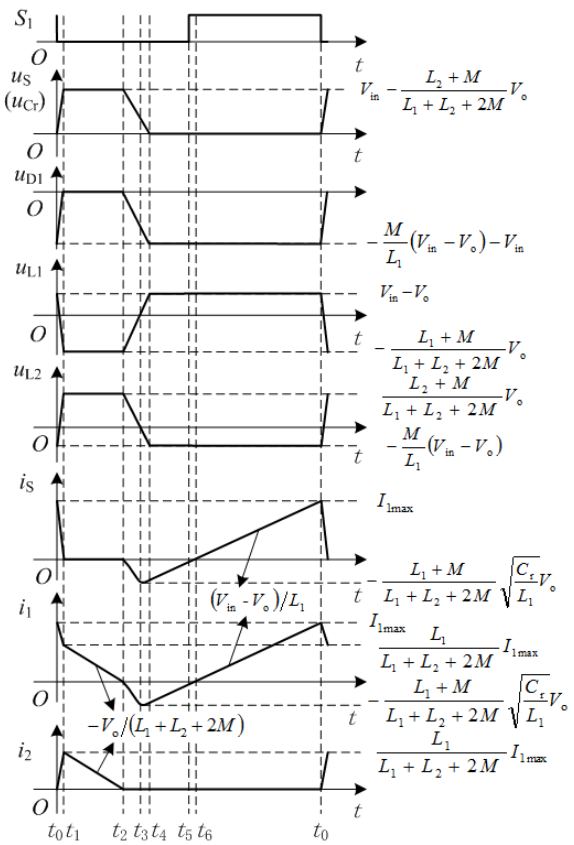

Fig. 2. Key ideal waveforms of the proposed ZVS-ZCS buck converter.

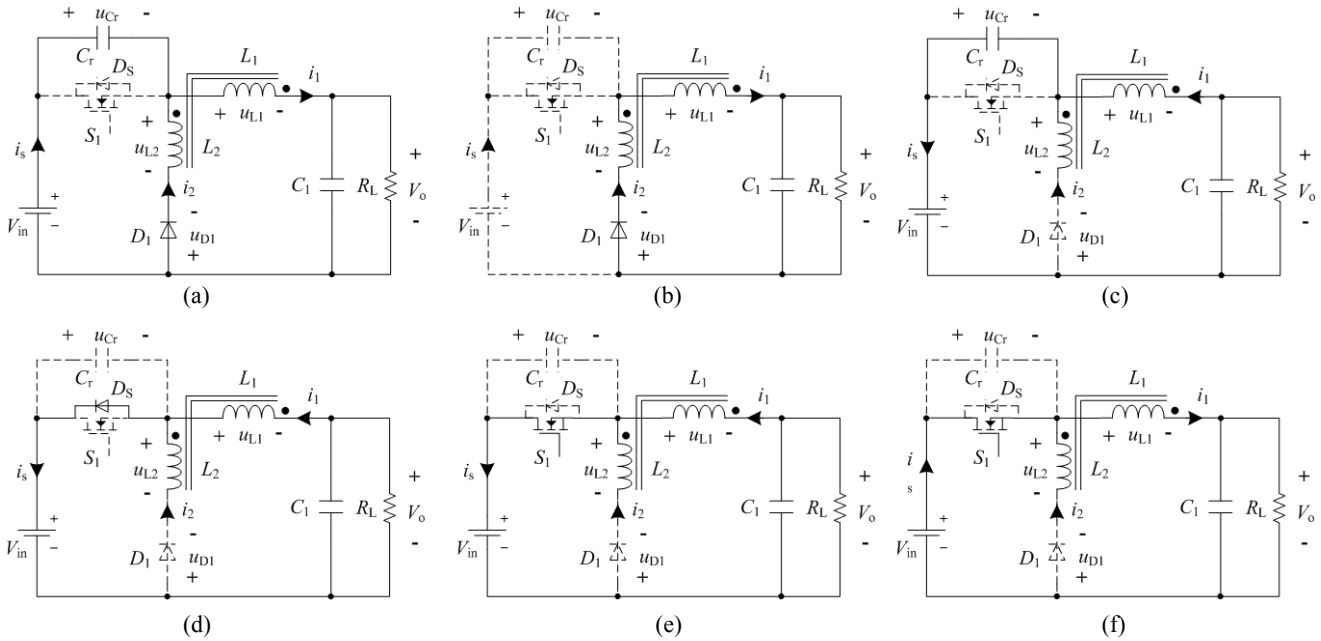

Fig. 3. Proposed ZVS-ZCS buck equivalent circuits of each operation mode. (a) Mode 1, t_0-t_1. (b) Mode 2, t_1-t_2. (c) Mode 3, t_2-t_4. (d) Mode 4, t_4-t_5. (e) Mode 5, t_5-t_6. (f) Mode 6, t_6-t_0.

condition, and the current of the coupled inductor L_1 reaches maximum value, i.e., $i_S = i_1 = I_{1max}$. At the same time, the freewheeling diode D_1 turns on automatically under a ZCS condition. After t_0, the coupled inductor L_1 discharges, and i_1 starts decreasing from I_{1max}, while the coupled inductor L_2, parasitic capacitor C_r charge, i_2, and u_{Cr} increase from zero. At t_1, i_S drops to zero, and i_1 and i_2 are equal to I_{t1}.The voltage across C_r reaches steady value, and the charging is completed.

According to Magnetism Chain Conservation Theorem, this process can have

$$L_1 I_{1\max} = (L_1 + L_2 + 2M) I_{t1} \tag{1}$$

where M is mutual inductance, and the coupling coefficient is about one, therefore $M = \sqrt{L_1 L_2}$.

Simplifying (1), i_1 and i_2 at t_1 can be obtained as follows:

$$i_1 = i_2 = I_{t1} = \frac{L_1}{L_1 + L_2 + 2M} I_{1\max} \tag{2}$$

2) Mode 2 [t_1-t_2, Fig. 3(b)]: The coupled inductor L_1 and L_2 discharge in this interval. After t_1, i_1 and i_2 are equal, and decrease linearly. The voltage across C_r remains steady value, and i_S is equal to zero.

The conduction voltage drop u_{D1} of the freewheeling diode D_1 is ignored, and based on KCL and KVL, we can obtain

$$\begin{cases} i_1 = i_2 \\ u_{L2} = u_{L1} + V_o \\ V_{in} = u_{L2} + u_{Cr} \end{cases} \tag{3}$$

The voltage equations of the coupled inductor L_1 and L_2 can be described as follows:

$$\begin{cases} u_{L1} = L_1 \dfrac{di_1}{dt} + M \dfrac{di_2}{dt} \\ u_{L2} = -L_2 \dfrac{di_2}{dt} - M \dfrac{di_1}{dt} \end{cases} \tag{4}$$

By substituting (4) into (3), the slopes of i_1 and i_2 are derived as follows:

$$k = \frac{di_1}{dt} = \frac{di_2}{dt} = -\frac{V_o}{L_1 + L_2 + 2M} \tag{5}$$

The slope of the filter inductor current of the conventional buck converter in this interval is equal to

$$k' = -(V_o / L_1) \tag{6}$$

Obviously, we can obtain

$$|k'| > |k| \tag{7}$$

Consequently, it demonstrates that the discharging of the proposed buck converter is slower than that of conventional buck converter in this mode, and it contributes to decrease the ripple of output voltage V_o.

Combining (3) and (4), the voltage across coupled inductor L_1, L_2, and parasitic capacitor C_r can be written as follows:

$$\begin{cases} u_{L1} = -\dfrac{L_1 + M}{L_1 + L_2 + 2M} V_o \\ u_{L2} = \dfrac{L_2 + M}{L_1 + L_2 + 2M} V_o \\ u_{Cr} = V_{in} - \dfrac{L_2 + M}{L_1 + L_2 + 2M} V_o \end{cases} \tag{8}$$

3) Mode 3 [t_2-t_4, Fig. 3(c)]: The resonance between the parasitic capacitor C_r and coupled inductor L_1 occurs in this

interval. At t_2, i_1 and i_2 are equal to zero. It provides a necessary condition for the freewheeling diode D_1 turned off under a ZCS condition. After t_2, the parasitic capacitor C_r discharges through coupled inductor L_1, and i_1 changes its direction and is equal to i_S. At t_3, i_1 reaches negative maximum value. Then, i_1 starts to decline negatively until the voltage u_{Cr} drops to zero at t_4.

Let us make an assumption that the output capacitor C_1 is large enough, or the output voltage V_o is constant. Based on KCL and KVL, we can obtain

$$\begin{cases} i_S = i_1 \\ V_{in} = u_{Cr} + u_{L1} + V_o \end{cases} \tag{9}$$

The current equation of coupled inductor L_1 and the voltage equation of parasitic capacitor C_r can be expressed as follows:

$$\begin{cases} i_S = C_r \dfrac{du_{Cr}}{dt} \\ u_{L1} = L_1 \dfrac{di_1}{dt} \end{cases} \tag{10}$$

Combining (9) and (10), the following resonant equation can be written as follows:

$$L_1 C_r \frac{d^2 u_{Cr}}{dt^2} + u_{Cr} = V_{in} - V_o \tag{11}$$

The initial conditions of the resonant circuit at t_2 are $i_1 = 0$, and $u_{Cr} = V_{in} - \dfrac{L_2 + M}{L_1 + L_2 + 2M} V_o$. Some assumptions are made in this interval as follows:

$$\omega_0 = 1/\sqrt{L_1 C_r} \tag{12}$$

$$Z_0 = \sqrt{L_1 / C_r} \tag{13}$$

$$U_0 = \frac{L_1 + M}{L_1 + L_2 + 2M} V_o \tag{14}$$

According to the abovementioned equations in this mode, i_1, i_S, and u_{Cr} are derived as follows:

$$\begin{cases} u_{Cr} = U_0 \cos\left(\omega_0 (t - t_2)\right) + V_{in} - V_o \\ i_1 = i_S = -\dfrac{U_0}{Z_0} \sin\left(\omega_0 (t - t_2)\right) \end{cases} \tag{15}$$

where the constraint condition is $t_2 \le t \le t_4$.

4) Mode 4 [t_4-t_5, Fig. 3(d)]: The anti-parallel diode D_S is turned on in this interval. At t_4, the discharging of parasitic capacitor C_r is completed, and u_{Cr} is equal to zero. After t_4, the anti-parallel diode D_S turns on. As a result, it makes u_{Cr} stay at zero. Meanwhile, i_1 is negative and is equal to i_S, which declines linearly. The conduction voltage drop of the anti-parallel diode D_S can be neglected, and based on KVL equation, the voltage u_{L1} across coupled inductor L_1 is given by

$$u_{L1} = V_{in} - V_o \tag{16}$$

Then, the slope of i_1 can be obtained as follows:

$$k = \frac{di_1}{dt} = \left(V_{in} - V_o\right) / L_1 \tag{17}$$

At the same time, the voltage u_{L2} across coupled inductor L_2 can be derived as follows:

$$u_{L2} = -M \frac{di_1}{dt} = -\frac{M}{L_1}\left(V_{in} - V_o\right). \tag{18}$$

According to KVL, the voltage u_{D1} of the freewheeling diode can be written as follows:

$$u_{D1} = u_{L2} - u_{L1} - V_o = -\frac{M}{L_1}\left(V_{in} - V_o\right) - V_{in}. \tag{19}$$

5) Mode 5 [t_5-t_6, Fig. 3(e)]: The switch S_1 is turned on, and the current i_1 is negative in this interval. Before t_5, the current i_1 flows through anti-parallel diode D_S, and the voltage u_{Cr} of the parasitic capacitor C_r is equal to zero. Therefore, a ZVS condition of the switch S_1 turned on can be obtained at t_5. After t_5, it is the same as Mode 4, except that i_1 flows through switch S_1. The current i_1 decreases negatively with the slope $\left(V_{in} - V_o\right)/L_1$ until it reaches zero at t_6.

6) Mode 6 [t_6-t_0, Fig. 3(f)]: The switch S_1 is turned on, and the current i_1 is positive in this interval. At t_6, the current i_1 changes its direction. After t_6, this mode is the same as Mode 4 and Mode 5, except that the current i_1 is positive. Then, i_1 increases linearly with the slope $\left(V_{in} - V_o\right)/L_1$ until switch S_1 turns off at t_0. At the end of this mode, the next operating cycle begins.

III. Soft Switching Analysis and Design Parameters

A. Analysis of the Soft Switching

The proposed buck converter can easily achieve ZCS conditions of the freewheeling diode D_1, as long as the coupled inductor L_1 is so small that it can reduce the current i_1 to zero and become negative, i.e., the coupled inductor L_1 works under a discontinuous conduction mode (DCM). Then, some assumptions are made as follows:

$$K = 2L_1 / RT_S \tag{20}$$

$$N = \sqrt{L_2 / L_1} \tag{21}$$

where R is load resistor, T_S is switching period, N is turn ratio, and the dimensionless parameter K is a measure of the tendency of a converter to operate in the DCM.

Therefore, the following formula must be satisfied to make the proposed converter operate under DCM

$$K < \frac{1}{\left(1 + N\right)^2}\left(1 - D\right) \tag{22}$$

where D is the duty cycle.

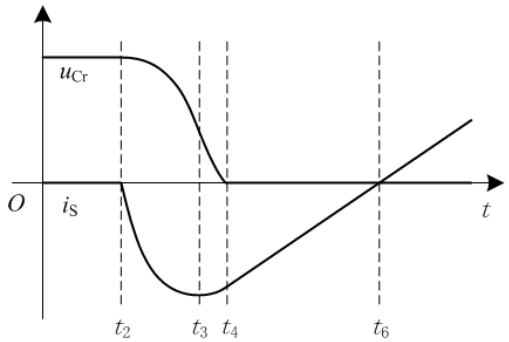

Fig. 4. ZVS condition analyses particularly.

However, to obtain ZVS conditions of the switch S_1, the switch S_1 must be turned on between t_4 and t_6, as shown in Fig. 4.

According to the voltage across parasitic capacitor C_r in equation (15), t_4 can be obtained as follows:

$$t_4 = \frac{1}{\omega_0}\left(\pi - \cos^{-1}\left(\frac{V_{in} - V_o}{U_0}\right)\right) + t_2 \tag{23}$$

Then, we can obtain

$$I_{t4} = -\frac{U_0}{Z_0}\sin\left(\pi - \cos^{-1}\left(\frac{V_{in} - V_o}{U_0}\right)\right) = -\frac{1}{Z_0}\sqrt{U_0^{\,2} - (V_{in} - V_o)^2} \tag{24}$$

where I_{t4} is the current i_S at t_4.

Consequently, ΔT that is between t_4 and t_6 can be derived as follows:

$$\Delta T = \frac{1}{\omega_0}\sqrt{\left(\frac{U_0}{V_{in} - V_o}\right)^2 - 1} \tag{25}$$

B. Design of the Proposed Circuits

As presented in formula (22), the coupled inductor L_1 must be chosen a small one to satisfy it. However, to achieve ZVS better, it demands ΔT as long as possible.

The voltage conversion ratio M_D is the ratio of the output to the input voltage of the converter, and can be obtained under DCM as follows:

$$M_D = V_o / V_{in} = \frac{2}{2 - (1+N)^2 + (1+N)\sqrt{(1+N)^2 + 4K/D^2}} \tag{26}$$

Thus, the equation (25) can be simplified as follows:

$$\Delta T = \frac{1}{\omega_0}\sqrt{\left(\frac{M_D}{(1 - M_D)(1+N)}\right)^2 - 1} \tag{27}$$

As we can see in equation (27), the ΔT is closely related to ω_0, i.e., the coupled inductor L_1 and resonant capacitor C_r. Therefore, when the design of the coupled inductor L_1 is completed, and the voltage conversion ratio M_D and turn ratio N are constant, it can be chosen a large resonant capacitor C_r to increase ΔT. But at the same time, the current i_1 at t_3 is $-U_0/Z_0$, which also increases. As a matter of fact, we expect to decrease the value of i_1 at t_3. Hence, the volume of C_r must be appropriate. The specific values and others parameter values are shown in Table I.

TABLE I
RELATED SPECIFICATIONS OF THE PROPOSED CONVERTER

Parameters	Values
Input voltage V_{in}	48V
Output voltage V_o	32V
Output power P_o	200W
Switching period T_S	20μs
Couple inductor L_1	5μH
Couple inductor L_2	5μH
parasitic capacitor C_r	440nF
filter capacitor C_1	220μF

IV. SIMULATION ANALYSIS

A. Soft Switching Waveforms of Simulation

To illustrate the operation of the proposed ZVS-ZCS buck converter, it has been accomplished through a simulation with Multisim software. Using the parameters in Table I, the soft-switching waveforms are obtained, in which the turn ratio N is equal to 1, as shown in Fig. 5.

The resonant circuit, which consists of the coupled inductor L_1 and parasitic capacitor C_r, provides a necessary condition for switch S_1 turned on under a ZVS condition. Furthermore, the ZVS condition of switch S_1 turned off is obtained by the parasitic capacitor C_r, as shown in Fig. 5(a). Since the proposed converter works under DCM, the current i_2 is equal to zero at the freewheeling diode D_1 both turned on and turned off. Therefore, the ZCS conditions of the freewheeling diode D_1 that is turned on and turned off are achieved, as shown in Fig. 5(b). The voltage u_{L1} and current i_1 of coupled inductor L_1 are supplied in Fig. 5(c).

B. Analysis of Power Losses

The power losses of the proposed ZVS-ZCS buck converter can be divided into three segments, i.e., switch losses, diode losses, and others. When the turn ratio N is equal to 1, power losses at different output power are shown in Fig. 6. As we can see in the figure, the main factors that affect the total efficiency of the proposed converter are the switch and diode losses.

As shown in Fig. 5(a), the switch losses are closely related to the voltage u_{Cr}, i.e., the switch losses will decrease as the voltage u_{Cr} declines and when the switch S_1 turns off. The

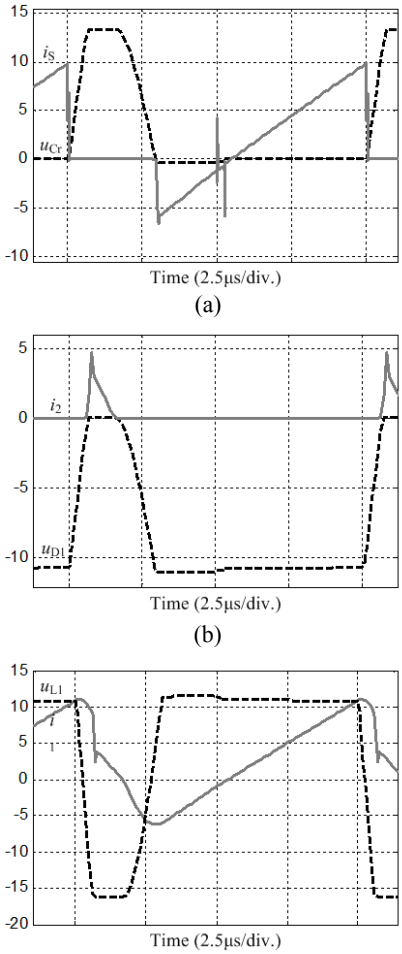

Fig. 5. The soft switching waveforms of simulation. (a) ZVS conditions of switch S_1 (magnification: voltage is 0.5 and current is 1). (b) ZCS conditions of freewheeling diode D_1 (magnification: voltage is 0.2 and current is 1). (c) The voltage and current of coupled inductor L_1 (magnification: voltage is 0.833 and current is 1).

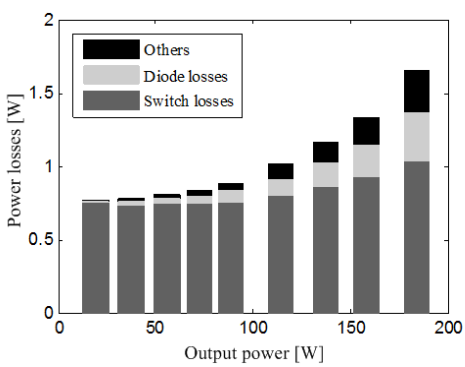

Fig. 6. Power losses of the proposed converter.

voltage of parasitic capacitor C_r in equation (8) can be simplified as follows:

$$u_{Cr} = V_{in} - \frac{1}{1+1/N} V_o \tag{28}$$

The normalized parameter u_{Cr_N} is

$$u_{Cr\_N} = 1 - \frac{NM_D}{1+N} \tag{29}$$

Similarly, Fig. 5(b) shows that the diode losses will reduce as the current i_2 declines at freewheeling diode D_1 turned on moment. The maximum value I_{1max} of the current i_1 at t_0 can be derived under hard-switching conditions as follows:

$$I_{1max} = DT_S(V_{in} - V_o)/L_1 \tag{30}$$

Therefore, the current i_2 of coupled inductor L_2 at t_1 in equation (2) can be simplified as follows:

$$I_{t1} = \frac{V_{in} - V_o}{(1+N)^2 L_1} DT_S. \tag{31}$$

Normalized Current I_{t1_N} is defined as

$$I_{t1\_N} = \frac{1 - M_D}{(1+N)^2} D. \tag{32}$$

The contours of u_{Cr_N} and I_{t1_N} are shown in Fig. 7(a) and (b), respectively, in which K is constant value. The x axis represents the duty cycle D, and the y axis represents the turn ratio N. As shown in Fig. 7, the increase of duty cycle D results in a decrease of u_{Cr_N}. However, I_{t1_N} increases first, then decreases, while u_{Cr_N} and I_{t1_N} will both decrease as the turn ratio N increases. In Fig. 8, the switch losses and freewheeling diode losses are presented with different turn ratio N at diverse output power, respectively. Both the switch losses and freewheeling diode losses can be decreased by increasing the turn ratio N. Hence, the total power losses can be decreased by increasing the turn ratio N, i.e., the overall efficiency of the proposed converter can be improved this way.

C. Evaluation of Output Voltage

The ripple of output voltage V_o, an important index to evaluate the performance of proposed buck converter, is affected by the slopes of i_1 and i_2 when the freewheeling diode D_1 turns on. The equation (5) can be simplified as follows:

$$k = -\frac{V_o}{(1+N)^2 L_1} \tag{33}$$

In any case, the value of coupled inductor L_1 is so small that the current i_1 can be negative. Hence, the ripple of output voltage also closely associates with the current i_1. At t_3, the negative maximum of the current i_1 is

$$I_{t3} = -\frac{L_1 + M}{L_1 + L_2 + 2M} \frac{V_o}{Z_0} = -\frac{V_o}{(1+N)Z_0} \tag{34}$$

According to the couple of equations above, when the coupled inductor L_1, parasitic capacitor C_r, and output voltage V_o are constant, $|k|$ and $|I_{t3}|$ will both decrease as turn ratio N increases. That is to say, the ripple of V_o can be decreased by increasing turn ratio N. In Table II, the ripples of V_o are presented at different turn ratio N by simulation.

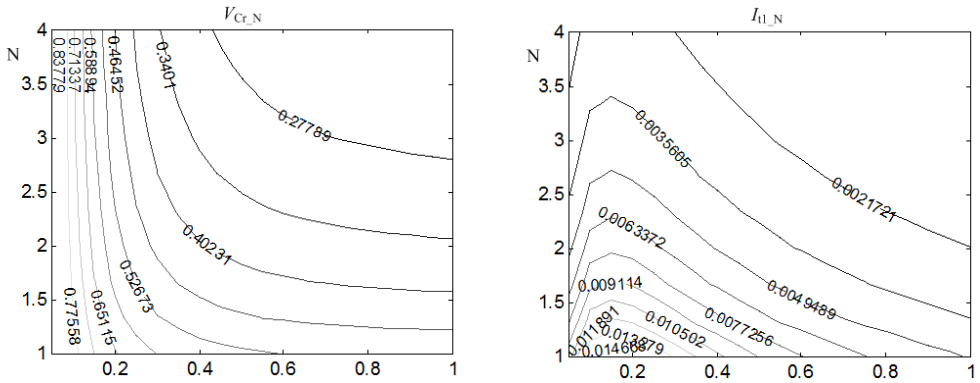

Fig. 7. Contour graphs of the proposed converter. (a) u_{Cr_N} contour graph. (b) I_{t1_N} contour graph.

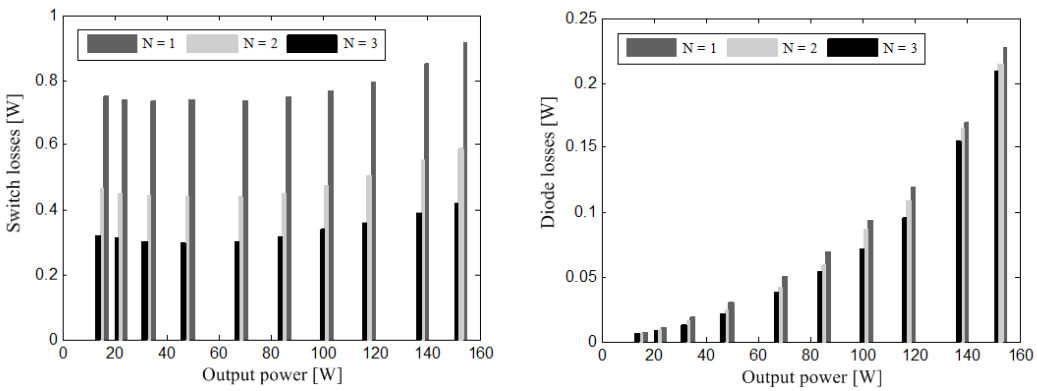

Fig. 8. Switch and freewheeling diode losses of the proposed converter. (a) Switch losses. (b) Freewheeling diode losses.

TABLE II
RIPPLE OF OUTPUT VOLTAGE AT DIFFERENT TURN RATIO

Turn ratio N	Ripple of V_o /mV
1	301
2	215
3	173
4	156

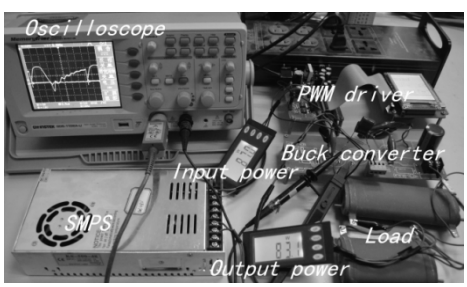

Fig. 9. The prototype of the proposed converter.

V. EXPERIMENTAL RESULTS

To verify the theoretical and simulated results of the proposed ZVS-ZCS buck converter, a 200-W and 50-kHz prototype has been built in the laboratory. The photograph of the proposed converter prototype is shown in Fig. 9. The used parameter values are the same as those specified in the simulation, and the semiconductors used are

- Switch S_1: MOSFET IRL2910S
- Freewheeling diode D_1: MBR30200PT.

A. Soft Switching Waveforms of Experiment

The experimental soft-switching waveforms of the proposed ZVS-ZCS buck converter at medium load, light load and full load are shown in Fig. 10, 11, and 12, respectively. It is presented that the ZVS operations of the switch S_1 at turned on and off moment are achieved in Fig. 10(a). The coupled inductor L_1 and parasitic capacitor C_r constitute a resonant circuit that provides a ZVS-turned on condition for the switch S_1. The parasitic capacitor C_r is parallel with the switch S_1, and makes a necessary condition for the switch S_1 turned off under a ZVS condition. In Fig. 10(b), the ZCS conditions of the freewheeling diode D_1 turned on and off also happen. Because of the proposed converter working under DCM, the current i_2 dropped to zero before the freewheeling diode D_1 turned off. Furthermore, the current i_2 keeps at zero until the freewheeling diode D_1 turns on. The experimental voltage u_{L1} and current i_1 of coupled inductor L_1 are shown in Fig. 10(c). In comparison to Fig. 11 and 12, the proposed buck converter can successfully achieve ZVS and ZCS conditions, as well.

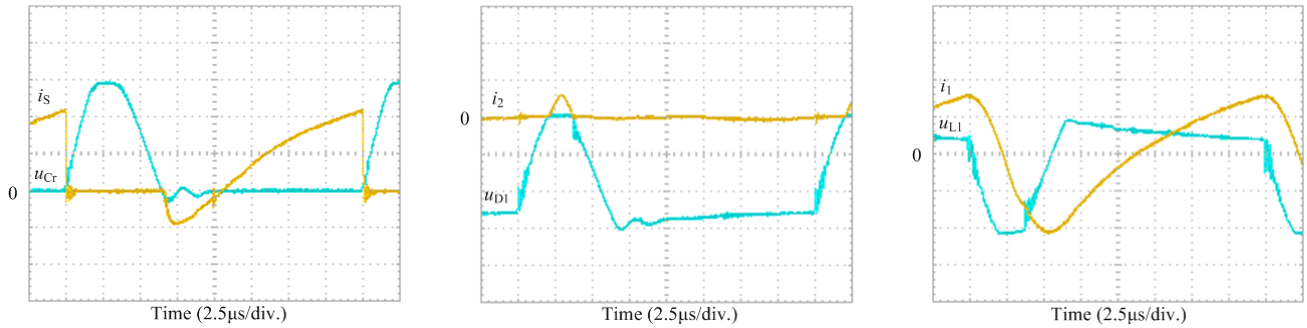

(a) (b) (c)

Fig. 10. Experimental waveforms at medium load. (a) ZVS conditions of switch S_1 (current i_S: 5A/div. and voltage u_{Cr}: 10V/div.). (b) ZCS conditions of freewheeling diode D_1 (current i_2: 5A/div. and voltage u_{D1}: 20V/div.). (c) The voltage and current of coupled inductor L_1 (current i_1: 5A/div. and voltage u_{L1}: 10V/div.).

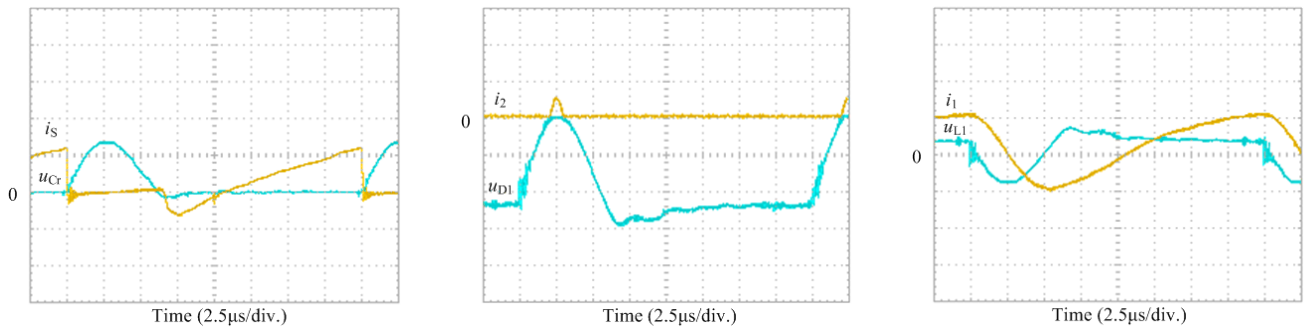

(a) (b) (c)

Fig. 11. Experimental waveforms at light load. (a) ZVS conditions of switch S_1 (current i_S: 5A/div. and voltage u_{Cr}: 20V/div.). (b) ZCS conditions of freewheeling diode D_1 (current i_2: 2A/div. and voltage u_{D1}: 20V/div.). (c) The voltage and current of coupled inductor L_1 (current i_1: 5A/div. and voltage u_{L1}: 20V/div.).

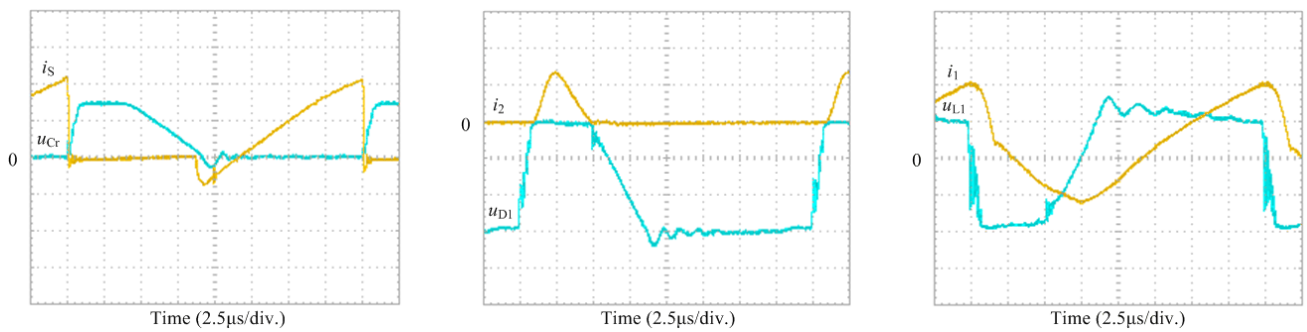

(a) (b) (c)

Fig. 12. The experimental waveforms at full load. (a) ZVS conditions of switch S_1 (current i_S: 10A/div. and voltage u_{Cr}: 20V/div.). (b) ZCS conditions of freewheeling diode D_1 (current i_2: 10A/div. and voltage u_{D1}: 20V/div.). (c) The voltage and current of coupled inductor L_1 (current i_1: 10A/div. and voltage u_{L1}: 10V/div.).

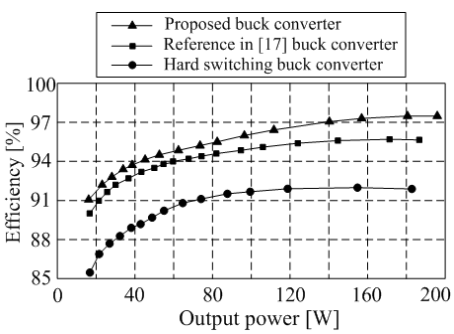

Fig. 13. Measured efficiency.

B. *Efficiency*

The efficiency curves of the buck converters are shown in Fig. 13. As we can observe in the figure, the overall efficiency values of the proposed buck converter are relatively high with respect to those of the rest buck converters. Moreover, the efficiency reaches 97.3% at full load. The figure also shows that even at light load (about 10% of the full power) the measured efficiency is as high as 91%.

VI. CONCLUSION

In this paper, a simple structure of ZVS-ZCS buck converter with coupled inductor has been proposed. Both the switch working under ZVS conditions and freewheeling diode working under ZCS conditions at turned on and off are achieved. The detailed theoretical analyses of the operating principle at steady state have also been provided. The main factors of power losses are discussed. The prototype of the proposed buck converter was built, and the simulation and experimental results confirm the related theoretical analyses. Since no additional component is added in this topology, the proposed converter presents a simple structure and also enjoys a very simple control method, as well as that of the conventional buck converter.

REFERENCES

[1] M. Jabbari, "Unified analysis of switched-resonator converters," *IEEE Trans. Power Electron.*, Vol. 26, No. 5, pp. 1364-1376, May 2011.

[2] I. Aksoy, H. Bodur and A. F. Bakan, "A new ZVT-ZCT-PWM DC-DC converter," *IEEE Trans. Power Electron.*, Vol. 25, No. 8, pp. 2093-2105, Aug. 2011.

[3] M. Jabbari and H. Farzanehfard, "New resonant step-down/up converters," *IEEE Trans. Power Electron.*, Vol. 25, No. 1, pp. 249-256, Jan. 2010.

[4] E. Adib and H. Farzanehfard, "Family of zero-current transition PWM converters," *IEEE Trans. Ind. Electron.*, Vol. 55, No. 8, pp. 3055-3063, Aug. 2008.

[5] S. Urgun, "Zero-voltage transition-zero-current transition pulse width modulation DC-DC buck converter with zero-voltage switching zero-current switching auxiliary circuit," *IET Power Electron.*, Vol. 5, No. 5, pp. 627-634, May 2012.

[6] M. Ilic and D. Maksimovic, "Interleaved zero-current-transition buck converter," *IEEE Trans. Ind. Appl.*, Vol. 43, No.6, pp. 1619-1627, Nov. 2007.

[7] A. Emrani and H. Farzanehfard, "Zero-current switching resonant buck converters with small inductors," *IET Power Electron.*, Vol. 5, No. 6, pp. 710-718, Jul. 2012.

[8] S. Pattnaik, A. K. Panda and K. K. Mahapatra, "Efficiency Improvement of Synchronous Buck Converter by Passive Auxiliary Circuit," *IEEE Trans. Ind. Electron.*, Vol. 46, No. 6, pp. 2511-2517, Nov. 2010.

[9] P. Das and G. Moschopoulos, "A comparative study of zero-current transition PWM converters," *IEEE Trans. Ind. Electron.*, Vol. 54, No. 3, pp. 1319-1328, Mar. 2007.

[10] M. R. Amini and H. Farzanehfard, "Switched resonator DC/DC converter with a single switch and small inductors," *IET Power Electron.*, Vol. 7, No. 6, pp. 1331-1339, Jan. 2014.

[11] C.-Y. Chiang and C.-L. Chen, "Zero-voltage-switching control for a PWM buck converter under DCM/CCM boundary," *IEEE Trans. Power Electron.*, Vol. 24, No. 9, pp. 2120-2126, Sep. 2009.

[12] W. Yu, J.-S. Lai, and S.-Y. Park, "An improved zero-voltage switching inverter using two coupled magnetics in one resonant pole," *IEEE Trans. Power Electron.*, Vol. 25, No. 4, pp. 952-961, Apr. 2010.

[13] H.-L. Do, "Zero-voltage-switching synchronous buck converter with a coupled inductor," *IEEE Trans. Ind. Electron.*, Vol. 58, No. 8, pp. 3440- 3447, Aug. 2011.

[14] Y. Berkovich and B. Axelrod, "Switched-coupled inductor cell for DC- DC converters with very large conversion ratio," *IET Power Electron.*, Vol. 4, No. 3, pp. 309-315, Mar. 2011.

[15] Lei Jiang, C. C. Mi, Li Siqi, Yin Chengliang and Li Jinchuan, "An improved soft-switching buck converter with coupled inductor," *IEEE Trans. Power Electron.*, Vol. 28, No. 11, pp. 4885- 4891, Nov. 2013.

[16] M. R. Amini and H. Farzanehfard, "Novel family of PWM soft-single-switched DC-DC converters with coupled inductors," *IEEE Trans. Ind. Electron.*, Vol. 56, No. 6, pp. 2108-2114, Jun. 2009.

[17] J.-H. Park and B.-H. Cho, "Nonisolation soft-switching buck converter with tapped-inductor for wide-input extreme step-down applications," *IEEE Trans. Circ. and Sys.*, Vol. 54, No. 8, pp. 1809-1818, Aug. 2007.

[18] J. J. Lee and B. H. Kwon, "DC-DC converter using a multiple-coupled inductor for low output voltages," *IEEE Trans. Ind. Electron.*, Vol. 54, No. 1, pp. 467-478, Feb. 2007.

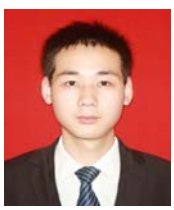

Xinxin Wei was born in Henan, China. He received his B.S. degree in Electronics Engineering from Zhongyuan University of Technology, Zhengzhou, China in 2013. He is currently a postgraduate student in the School of Electronics Engineering, Chongqing University. His research interest area is power electronics in general, especially the analysis and design of switching power converters, high-frequency power conversion and soft-switching converters.

Ciyong Luo was born in Anhui in 1973. He received his B.S and M.S degrees in Automatic Control and Ph.D. degree in Electronics Engineering from Chongqing University, Chongqing, China, in 1995, 1998, and 2005, respectively. From January 2011 to January 2012, he was with the Department of Automatic Control and Systems Engineering, University of Sheffield, Sheffield, UK, as a Visiting Scholar. He is currently an Associate Professor in the School of Electrical Engineering, Chongqing University. His research interests include the modeling, design, and control of power converters, soft-switching power converters, the modeling and analysis of the dynamical behavior of switching DC-DC converters, and power-factor correction circuits.

Hang Nan was born in Hubei in 1989. He received his B.S. degree in electrical engineering from Hubei University of Technology, Wuhan, China in 2013. He is currently a postgraduate student in the School of Electronics Engineering Chongqing University. His research interests include the modulation methods of switching power converters, power electronics, and especially, DC-DC converters.

Yinghao Wang was born in Hebei in 1989. He received his B.S. degree in electrical engineering from Chongqing University, Chongqing, China in 2013. He is currently a postgraduate student in the School of Electronics Engineering Chongqing University. His research interests include the modulation methods of switching power converters, and the modeling and analysis of the dynamical behavior of switching DC-DC converters.